Asian Journal of Water, Environment and Pollution. 2026;23(2):025380292.
doi: 10.36922/AJWEP025380292

ORIGINAL RESEARCH ARTICLE

Effectiveness of raw and activated laterite in removing lead and copper from aqueous solutions: A kinetic and thermodynamic study

Corneille Bakouan[1,2,3]*, Ollé Rodrigue Kam[2], Anne-Lise Hantson[3], and Boubié Guel[2]

[1]Research and Development Laboratory, Faculty of Science and Technology, Lédéa Bernard Ouédraogo University, Ouahigouya, Burkina Faso
[2]Laboratory of Molecular Chemistry and Materials, Faculty Exact and Applied Science, Joseph Ki-Zerbo University, Ouagadougou, Burkina Faso
[3]Department of Chemical and Biochemical Engineering, Faculty of Polytechnic, University of Mons, Mons, Belgium
***Corresponding author**: Corneille Bakouan (corneille.bakouan@uohg.gov.bf)

Received: September 16, 2025; 1st revised: November 1, 2025; 2nd revised: November 24, 2025; Accepted: November 27, 2025; Published online: December 24, 2025

Abstract: The growing interest in local materials as natural adsorbents stems from their abundance, low cost, and eco-friendliness, offering an effective, economical, and sustainable alternative to commercial options. The present work investigates the removal performance of lead (Pb^{2+}) and copper (Cu^{2+}) ions from synthetic aqueous solutions using both raw and activated laterite (KN-Ac) under batch conditions. The experiments were carried out to examine the effects of contact time, adsorbent dose, temperature, pH, and initial metal-ion concentration. High determination coefficients obtained from the pseudo-second-order kinetics and Langmuir isotherm models indicate that these models reliably describe the experimental adsorption behavior of the metal ions. The diffusion model-adjusted data revealed that adsorption occurred rapidly at the beginning, with fast adsorption on the outer surface followed by slower adsorption controlled by intraparticle diffusion. The KN-Ac, designated KN-Ac, proved to be highly effective in removing both heavy metals, achieving removal percentages of 97.81 ± 0.23% (4.07 ± 0.01 mg/g) for Pb^{2+} and 94.24 ± 0.18% (1.18 ± 0.02 mg/g) for Cu^{2+} at an initial concentration of 10 mg/L. The ΔG values obtained for the metal ions were all negative, indicating that the adsorption process is feasible and spontaneous for Pb(II) and Cu(II) ions on the adsorbents, following the order of thermodynamic stability: Pb^{2+}(KN-Ac) > Cu^{2+}(KN-Ac) > Pb^{2+}(raw laterite [KN]) > Cu^{2+}(KN) in the temperature range of 303–333 K. The positive ΔH values for all metal ions suggest that adsorption onto the adsorbents is endothermic and involves physisorption. The energy values derived from the Dubinin–Radushkevich equation are all below 8 kJ/mol, indicating that the adsorption of Pb^{2+} and Cu^{2+} is physical in nature. Furthermore, the Fourier transform infrared spectra of adsorbent residues loaded with heavy metals show no changes compared to the spectra of the unloaded adsorbents, confirming physisorption as the main adsorption mechanism.

Keywords: Heavy metals; Removal; Groundwater; Wastewater; Laterite

1. Introduction

Heavy metal accumulation in environmental compartments, such as water and soil may have detrimental effects on both ecosystems and human populations. The presence of elevated levels of heavy metals in water and soil poses risks to ecosystems and human health.[1,2] Their occurrence in waterways, lakes, and groundwater reservoirs has led to several serious health problems. Contamination of water and soil by heavy metals can originate from both natural and anthropogenic sources. Natural sources include soil erosion, forest fires, volcanic eruptions, biogenic processes, and the release of sea salt.[3,4] Anthropogenic contamination occurs through activities, such as mining operations, the use of fertilizers, herbicides, and pesticides, and the irrigation of agricultural land with untreated wastewater and industrial effluents.[1,5-7]

Large areas of water and land have been polluted by inorganic contaminants, such as pesticides, fertilizers, sludge, and municipal waste, which often contain toxic metals. Their carcinogenic properties pose risks to both aquatic ecosystems and human health, making their presence in water a significant environmental concern.[4,8] Although some heavy metals serve as essential trace elements for human growth and development, prolonged exposure to elevated levels can induce a range of diseases.[5,9]

Copper (Cu) and lead (Pb) exhibit toxic properties, and their discharge into the aquatic environment is increasing significantly due to rapid urbanization and industrialization worldwide. They are released into the environment by battery and paint manufacturing industries, as well as metallurgical, mining, and smelting industries.[8] Consumption of water containing Cu (2 mg/L)[9,10] and Pb (0.01 mg/L)[9] above the World Health Organization (WHO) acceptable limits is hazardous to human health and can cause diseases, such as Alzheimer's disease, headaches, vomiting, lung disease, nausea, stomach cramps, brain disorders, liver cirrhosis, intestinal irritation, liver damage, kidney failure, and osteoporosis.[4,8,11]

In natural waters, Pb mainly exists in its soluble divalent ionic form, Pb^{2+}, and as aqueous carbonate species ($PbCO_3$[aq]). Speciation analyses show that in drinking water at pH 6.5–8.5, divalent Pb^{2+} and monovalent Pb hydroxide ($Pb(OH)^+$) predominate. Under alkaline conditions, Pb primarily occurs as $Pb(OH)_4^{2-}$ and $Pb(OH)_3^-$. For example, organic Pb compounds can be metabolized by the liver, whereas inorganic Pb tends to circulate between the bloodstream and various body tissues without undergoing such metabolism.[12]

Cu^{2+} and Pb^{2+} ions are non-biodegradable, and once discharged, they can accumulate in living organisms, adversely affecting all forms of life. It is therefore important to reduce their concentrations in drinking water and/or wastewater below WHO limits to mitigate their harmful effects.[8] Several treatment techniques have been used to remove heavy metal ions from aquatic environments, such as adsorption, ion exchange, coagulation/flocculation, chemical precipitation, electrocoagulation, photodegradation, and electrochemical oxidation.[10,13-19] Nonetheless, methods, such as chemical precipitation, coagulation/flocculation, ion exchange, reverse osmosis, photodegradation, and electrochemical oxidation possess inherent limitations,[10,13,19] including high cost, hazardous waste generation, inefficiency, and high energy consumption. Among these techniques, adsorption is considered one of the most effective due to its low operating cost, simplicity, high removal capacity, and environmentally friendly nature.[6,14] However, further research is required to identify locally available adsorbents suitable for possible environmental applications, particularly for the removal of heavy metals from water. Low-cost adsorbents are generally preferred for removing heavy metals from aqueous solutions and contaminated water. Consequently, the search for new, inexpensive, and highly effective materials for removing heavy metals (Cu and Pb) from water and industrial effluents is of significant environmental interest. Numerous researchers have evaluated the effectiveness of various adsorbents for removing Cu^{2+} and Pb^{2+} from aqueous solutions, including natural and modified bentonite,[14,20,21] smectic clay,[22,23] natural and modified clay,[16,24-27] natural zeolite,[28] montmorillonite and illite,[29,30] humic acid,[31] treated laterites.[12-14,32]

Laterite is a widely used adsorbent consisting of fine-grained, light-textured red, brown, and yellow residual soils, as well as cemented soils that form on rock surfaces through decomposition.[33] Laterite is abundant in Burkina Faso and can be utilized for the removal of toxic metals. It carries a positive charge under acidic and neutral conditions and has been extensively employed to eliminate various toxic anions, including anionic heavy metals.[17,34,35] However, the removal of cationic species is not favored at reactive sites due to electrostatic repulsions between the positively charged laterite surface and the cations. Therefore, to increase the efficiency of cation removal by adsorption, modification of the laterite surface is necessary.[13]

The main objectives of this study were to: (i) Activate raw laterite (KN) with acid to increase its specific surface area; (ii) determine the sorption capacities of KN and activated laterite (KN-Ac) for removing Pb^{2+} and Cu^{2+}; and (iii) elucidate the adsorption mechanisms of Pb^{2+} and Cu^{2+} at the laterite surface/aqueous medium interface through Fourier transform infrared spectroscopy (FTIR) characterization before and after adsorption.

2. Materials and methods

2.1. Materials

2.1.1. Origin of laterite

The laterite sample was collected in the region of Kaya, located 100 km from Ouagadougou, at the following coordinates: 13°07'13.47' North and 1°06'52.28' West. The sample was ground to a particle size ≤180 µm before being used in the batch adsorption experiments.

2.1.2. Chemicals

All solutions used in this study were prepared using Milli-Q water with a resistivity of 18.2 MΩ·cm. Stock solutions of 1,000 mg/L Pb^{2+} and Cu^{2+} were prepared from $Pb(NO_3)_2$ (≥99%, Merck, Germany) and $Cu(NO_3)_2 \cdot 3H_2O$) (≥99%, Merck), respectively, and stored at 4°C. These stock solutions were diluted to obtain the working aqueous solutions of Pb^{2+} and Cu^{2+} for the batch tests. The reagents nitric acid (HNO_3; 69%, Merck) and sodium hydroxide (NaOH; 99%, VWR, USA) used for pH adjustment, as well as hydrochloric acid (HCl; 37%, VWR) used for chemical modification of laterite, were all of analytical grade.

2.2. Materials and methods

2.2.1. Characterization of the adsorbent

The characterization of KN was described in our previous study.[36] The analysis revealed that the laterite sample contains major components, including quartz (SiO_2), kaolinite ($Al_2Si_2O_5(OH)_4$), hematite (Fe_2O_3), and goethite (FeO[OH]), and is rich in Fe_2O_3 (20.8%) and aluminum oxide (Al_2O_3; 14.09%).[36] FTIR analyses were performed using a Shimadzu FTIR-8400S instrument to obtain the infrared spectra of the samples before and after adsorption of the different metals, using potassium bromide pellets containing 2% by weight of laterite.

2.2.2. Activation of laterite

For the acid activation of KN, experiments were carried out by adapting the protocols proposed by Karki *et al*.[37] and Chatterjee and De.[38] In a 1 L glass container, 100 g of KN with particle sizes ranging from 0.106 to 0.180 mm was treated with 200 mL of 4 mol/L HCl and stirred for 4 h at 85 ± 5°C. After stirring, the solid phase was separated from the supernatant and rinsed with 400 mL of distilled water. A 2 mol/L NaOH solution was subsequently added and mixed at ambient temperature to adjust the final pH to between 6.5 and 7.5. The mixture was stirred for 3 h and left to stand for 1 day to allow decantation of the clear supernatant. The wet solid material was filtered through Whatman Grade 512½ qualitative cellulose filter paper, thoroughly washed several times with distilled water, dried in an oven at 60°C for 3 h, and then air-dried to obtain acid-modified KN-Ac.

The purpose of acid activation is partial dealumination, which increases the specific surface area of the laterite and enhances its ability to adsorb heavy metals. Under alkaline pH conditions, the surface charge of laterite becomes negative, thereby promoting the adsorption of heavy metals, such as Pb, Cu, and cadmium (Cd).[12]

2.2.3. Evaluation of the pH-dependent behavior of laterite before and after modification

Analyzing the behavior of an adsorbent in sodium chloride (NaCl) solutions across different pH levels before adsorption helps evaluate its stability and anticipate its performance under varying environmental conditions. To assess the behavior of KN and KN-Ac under different pH conditions, the procedure described by Chaari et *al*.[39] was followed. Ten flasks containing 50 mL of NaCl solution (0.01 mol/L) were prepared, and the pH was adjusted from 2 to 11 using either HNO_3 (0.2 mol/L) or NaOH (0.2 mol/L). Subsequently, 0.05 g of KN or KN-Ac was added to each flask. The mixtures were stirred for 24 h at 20 ± 2°C, after which the final pH values were recorded.

2.2.4. Batch adsorption experiments

Batch adsorption studies were performed to assess the removal efficiency of Pb^{2+} and Cu^{2+} by KN and KN-Ac at room temperature. These experiments aimed to determine the optimal values of parameters, including equilibrium time, adsorbent dose, and solution pH. A Consort C3010 multiparameter device (Fisher Scientific, USA) was used for pH measurements. Known masses of adsorbents were added to 250 mL polyethylene bottles containing 50 mL of Pb^{2+} and/or Cu^{2+} solution.

The mixtures were stirred at room temperature (20 ± 2°C) using a Heidolph REAX 20 mechanical shaker (Germany) and then centrifuged using a

BECKMAN J2-MI centrifuge (USA) at 1,308 g (radial centrifugal acceleration) for 15 min. The supernatants were filtered using nylon membranes with a diameter of 25 mm and a retention threshold of 0.45 µm.

Residual concentrations of Pb^{2+} and Cu^{2+} were quantified using an inductively coupled plasma optical emission spectrometer (PerkinElmer Optima 8300, USA). All experiments were performed in triplicate, with a variability of <5%. The amount of metal ions adsorbed at time t (q_t, [mg/g]) and at equilibrium (q_e, [mg/g]), as well as the percentage of adsorption (Ads[%]) were calculated using Equations 1-3.

$$q_t\left(\frac{mg}{g}\right)=\left(\frac{C_0-C_t}{m}\right)\times V \quad (1)$$

$$q_e\left(\frac{mg}{g}\right)=\left(\frac{C_0-C_e}{m}\right)\times V \quad (2)$$

$$Ads(\%)=\left(\frac{C_0-C_e}{C_0}\right)\times 100 \quad (3)$$

where q_t and q_e represent the amounts of metal adsorbed per unit mass of adsorbent (mg/g) at time t and at equilibrium, respectively; Ads(%) denotes removal efficiency; C_0 is the initial metal ion concentration (mg/L); C_t and C_e are the metal ion concentrations at time t and at equilibrium (mg/L); V is the total solution volume (L); and m corresponds to the adsorbent mass (g).

2.2.4.1. Effect of contact time

The influence of contact time on the adsorption of heavy metals by laterite was studied by varying the contact time from 5 to 90 min at 20 ± 2°C. To determine the optimal retention time, static tests were carried out on KN and KN-Ac at sample pH values of 5.34 ± 0.01 and 5.54 ± 0.07, respectively. A constant adsorbent dose was applied: 2.0 g of laterite/L for Pb^{2+} and 4.0 g of laterite/L for Cu^{2+} in 50 mL of solution containing 10 mg/L of heavy metal ions.

2.2.4.2. Effect of adsorbent dose

The influence of laterite dose on the adsorption of toxic metals was evaluated under equilibrium conditions at 20 ± 2°C. Working solutions of 10 mg/L of Pb^{2+} or Cu^{2+} (pH = 5.34–5.54) were mixed with varying masses of laterite in 50 mL. Adsorbent masses ranged from 0.4 g/L to 3.2 g/L for Pb^{2+} and 0.8 g/L to 16 g/L for Cu^{2+}.

2.2.4.3. Effect of pH

The influence of pH was examined by adjusting the pH of Pb^{2+} and Cu^{2+} solutions using diluted HNO_3 (0.2 mol/L) and NaOH (0.2 mol/L) at a temperature of 20 ± 2°C.

To avoid precipitation of Cu^{2+} and Pb^{2+} hydroxides, which could hinder the adsorption process, the initial pH of the solution was selected within the range of 2.0–6.0.

A mass of 0.12 g of adsorbent was brought into contact with 10 mg/L of Pb^{2+}, and 0.4 g with 10 mg/L of Cu^{2+} in 50 mL of solution. The mixtures were stirred for 1.5 h, and the equilibrium quantities of Pb^{2+} or Cu^{2+} adsorbed, q_e (mg/L), were evaluated using Equation 2.

2.2.4.4. Influence of initial concentration of Pb^{2+} and Cu^{2+}

The experiment was carried out by varying the initial concentration of Pb^{2+} and Cu^{2+} (pH = 5.34–5.54) from 5 to 40 mg/L at 20 ± 2°C. To each flask containing a solution of Pb^{2+} solution, 0.12 g of adsorbent was added, and 0.4 g of adsorbent was added to flasks containing Cu^{2+} solution in 50 mL. The mixtures were agitated for 1.5 h, and the equilibrium amount of Pb^{2+} or Cu^{2+} adsorbed per gram of adsorbent (q_e) was determined using Equation 2.

2.2.4.5. Influence of temperature

To assess the influence of temperature and to determine thermodynamic parameters, the amounts of Pb^{2+} and Cu^{2+} removed by the adsorbents were evaluated at pH 5.34–5.54 and at temperatures of 303, 313, 323, and 333 K. A mass of 0.12 g of laterite in 50 mL of 10 mg/L Pb^{2+} solution and 0.4 g of laterite in 50 mL of 10 mg/L Cu^{2+} solution were placed in a water bath for 1.5 h at 200 rpm. The equilibrium amount ($q_{e)}$ of Pb^{2+} or Cu^{2+} adsorbed per gram of adsorbent at each temperature was evaluated using Equation 2.

2.2.4.6. Co-adsorption of Pb^{2+} and Cu^{2+}

Pb^{2+} and Cu^{2+} were combined in the binary adsorption system at varying concentrations, in contrast to the single-metal adsorption systems. A volume of 50 mL of solution containing 10 mg/L of both Pb^{2+} and Cu^{2+} at pH 5.34–5.54 was prepared and contacted with 0.12 g of each adsorbent. The mixtures were stirred at 20 ± 2°Cfor 1.5 h, and the adsorption rate of each heavy metal was evaluated using Equation 3.

3. Results and discussion

3.1. Characterization of laterite

The laterite used in this study is a reddish-brown mineral composed of major oxides: Fe_2O_3 (20.8%), Al_2O_3(14.09%), and SiO_2 (50.16%).[36] The cation exchange capacity of KN was 52.3 ± 2.3 cmol(+)/kg. The surface area and pore volume measured by the Brunauer–Emmett–Teller method were 58 m^2/g and 0.14 cm^3/g, respectively.[36] A detailed composition of the laterite and its mineral characteristics can be found in our previous study.[36]

Figure 1 shows the nitrogen adsorption–desorption isotherms of the acid-activated sample. The surface area and pore volume were 75.14 m^2/g and 0.89 cm^3/g, respectively. The increase in the specific surface area of laterite after activation is attributed to a combination of factors, such as increased porosity, reduced particle size, and removal of impurities.

Assessing how adsorbents respond to different pH levels helps determine their surface charge characteristics, which directly affect electrostatic interactions with target metal ions. Such insight is crucial for selecting suitable pH conditions to enhance adsorption efficiency across diverse aqueous environments.[40,41]

Figure 2 shows that at pH values ≤5 for KN-Ac and ≤6 for KN, the equilibrium pH exceeds the initial pH, indicating surface protonation of the respective materials. This favors anion adsorption, while cation uptake is hindered due to electrostatic repulsion and competition with hydronium ions (H_3O^+). Similar trends were observed by Chu et *al*.[42] during the adsorption of Pb^{2+} and Cu^{2+} on both raw and arginine-modified montmorillonite. In contrast, at pH levels above 5, the equilibrium pH falls below the initial value, indicating surface deprotonation. This Pbs to a reduced H_3O^+ concentration and an increased availability of negatively charged sites, thereby enhancing the electrostatic attraction of metal cations to the adsorbent surface.

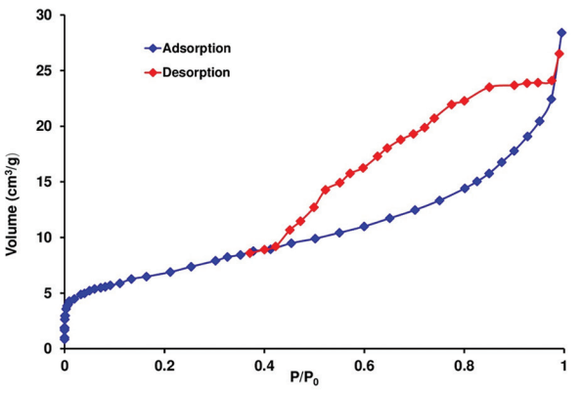

Figure 1. Nitrogen adsorption/desorption isotherms of activated laterite

3.2. Batch adsorption

3.2.1. Influence of contact time

The information acquired from the adsorption of Pb^{2+} and Cu^{2+} on KN and KN-Ac adsorbents is presented in Figure 3. The amount of each metal adsorbed indicates a strong affinity of the adsorbents for the metal ions from the 1st min of contact. As shown in Figure 3, the percentage removal of the metal ions (Cu^{2+} or Pb^{2+}) increased with time until equilibrium was reached after 30 min.

The quantities adsorbed after 30 min were 4.75 mg/g for KN-Ac (94.97%) and 2.89 mg/g of KN (57.82%) for Pb^{2+}, and 1.25 mg/g of KN-Ac (50.02%) and 0.69 mg/g of KN (27.70%) for Cu^{2+}. Increasing the contact time beyond 30 min had no significant effect on the amounts of metals adsorbed.

Initially, Pb^{2+} or Cu^{2+} adsorption was rapid due to the large number of active sites available on the adsorbents and the high concentration gradient. Once the active adsorbent surfaces began to be covered with cations, the adsorption rate slowed down and gradually approached a steady state.[43-46] The gradual slowing down of the adsorption process up to 90 min is attributed to the decreasing concentration gradient and the saturation of active binding sites of the adsorbents.[47]

The ionic radius of Pb^{2+} is approximately 1.20 Å, while that of Cu^{2+} is approximately 0.73 Å. However, ion adsorption depends more on their hydrated ionic radius than on the bare ionic radius. The diffusion rate of an ion in solution, essential for adsorption,

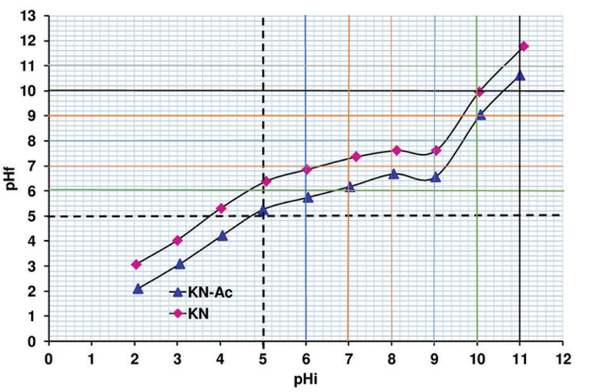

Figure 2. Behavior of raw laterite (KN) and activated laterite (KN-Ac) adsorbents as a function of pH

Notes: pHf: Final pH; pHi: Initial pH of the sodium chloride solution.

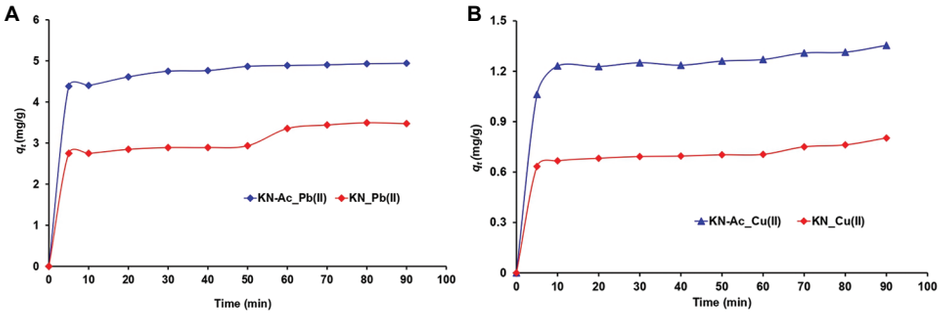

Figure 3. Effect of contact time on the adsorption of (A) lead (Pb[II]) and (B) copper (Cu[II]) on activated laterite (KN-Ac) and raw laterite (KN)

Note: q_t: The amount of metal adsorbed per unit mass of adsorbent at time t

is inversely proportional to its hydrated ionic radius (charge/naked ionic radius), which is influenced by the ion's charge density. A higher charge density results in increased hydration due to a stronger attraction to water molecules. Although Cu^{2+} has a smaller bare ionic radius than Pb^{2+}, its charge density is significantly higher, leading to greater hydration and a larger hydrated ionic radius. Consequently, hydrated Pb^{2+}, being smaller than hydrated Cu^{2+}, encounters less resistance in solution and has higher ionic mobility. This greater mobility enhances its transport from the solution to the adsorbent surface.

As a result, Pb^{2+} is adsorbed more efficiently than Cu^{2+} on the lateritic adsorbents KN-Ac and KN. The higher percentage of Pb^{2+} removal indicates a greater affinity of this ion for the adsorption sites of the laterite. This increased affinity, combined with its greater mobility due to its smaller hydrated ionic radius, explains the preferential adsorption of Pb^{2+} over Cu^{2+}. Similar results have been reported by other researchers for the adsorption of Pb^{2+} and Cu^{2+} on clays, zeolites, and laterites.[48-52]

Therefore, in subsequent tests, a contact time of 90 min was used. This ensures that all heavy metal ions can be adsorbed onto the adsorbents within 90 min.

3.2.2. Adsorption kinetics

To thoroughly investigate the adsorption dynamics and identify the rate-limiting steps, three kinetic models were applied: the pseudo-first-order model, the pseudo-second-order model, and the Weber–Morris intraparticle diffusion model. These models are described by Equations 4-6.[10,42]

$$ln(q_e - q_t) = lnq_e - k_1 \times t \quad (4)$$

$$\frac{t}{q_e} = \frac{1}{k_2 \times q_e^2} + \frac{1}{q_e} \times t \quad (5)$$

$$q_t = k_i \times \sqrt{t} + C_{ip} \quad (6)$$

where q_e (mg/g) and q_t (mg/g) represent the quantities of heavy metals adsorbed at equilibrium and at time t (min), respectively; $k_1(min^{-1})$ and k_2(g/mg.min) represent the pseudo-first-order and pseudo-second-order rate constants; C_{ip} (mg/g) is the intercept; and k_i ($mg/g.min^{½}$) is the intraparticle diffusion rate constant.

The plots of these kinetic models are shown in Figure 4, and Table 1 presents the parameters derived from them. The coefficient of determination ($R^2 \geq 0.98$) for the pseudo-second-order model was higher, and the calculated q_e values agreed well with the experimental values (Table 1). This better fit indicates that the adsorption kinetics of Pb^{2+} and Cu^{2+} on the adsorbents follow a pseudo-second-order model, suggesting chemical adsorption involving electron exchange between the adsorbent and adsorbate.[44,53]

The adsorption process also involves intraparticle diffusion, as indicated by the linearity of the plot of $q_t = f(\sqrt{t})$ (Figure 4C), with the parameters ki and C_{ip} listed in Table 1. Intraparticle diffusion is the predominant control step if the line passes through the origin. If it does not pass through the origin, intraparticle diffusion is not the only controlling step, and other processes also influence the adsorption rate.[54]

In this study, the plots (Figure 4C) do not intersect the origin, indicating that intraparticle diffusion contributes to the rate-limiting step of the adsorption process but is not the sole mechanism controlling adsorption.[54,55] Similar observations have been reported by Khater *et al.*[54] for the adsorption of heavy metals (Pb, Cu, nickel) on activated carbon and by Wu et *al.*[55] for the removal of Pb^{2+} and Cd^{2+} on manganese dioxide.

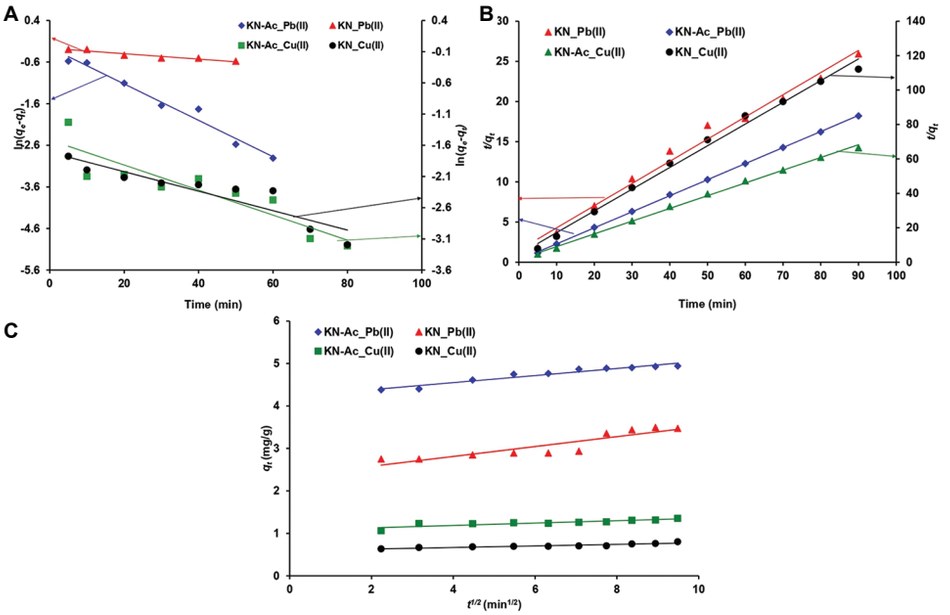

Figure 4. Adjustment of kinetic results according to (A) the pseudo-first-order model, (B) the pseudo-second-order model, and (C) the Weber–Morris intraparticle diffusion model

Note: q_t and q_e: The amounts of metal adsorbed per unit mass of adsorbent at time t and at equilibrium, respectively. Abbreviations: Cu(II): Copper; KN: Raw laterite; KN-Ac: Activated laterite; Pb(II): Lead.

Table 1. Kinetic parameters and correlation coefficients for the adsorption of lead (Pb[II]) and copper (Cu[II])

Models	Parameters	Pb (II)		Cu (II)	
		KN-Ac	KN	KN-Ac	KN
Pseudo- first-order	k_1 (min^{-1})	0.044	0.006	0.02	0.016
	$q_{e—cal}$ (mg/g)	0.778	0.765	0.219	0.180
	q_{e_exp} (mg/g)	4.942	3.494	1.354	0.803
	R^2	0.976	0.926	0.821	0.847
Pseudo-second- order	k_2 (g/mg.min)	0.142	0.050	0.331	0.346
	$q_{e—cal}$ (mg/g)	5.005	0.793	1.351	0.793
	q_{e_exp} (mg/g)	4.942	0.803	1.354	8.03
	R^2	0.999	0.987	0.998	0.993
Intraparticle diffusion	k_i (mg/g·$min^{1/2}$)	0.083	0.116	0.028	0.019
	C_{ip} (mg/g)	4.216	2.347	1.075	0.591
	R^2	0.943	0.821	0.768	0.860

Notes: q_e: The calculated (cal) and expected (exp) amounts of metal adsorbed per unit mass of adsorbent at equilibrium. C_{ip} (*mg*/*g*) is the intercept.
Abbreviations: KN: Raw laterite; KN-Ac: Activated laterite; Cu (II): Copper; Pb (II): Lead.

3.2.3. Influence of adsorbent dose

Determining the optimal adsorbent dose is crucial, as it determines the adsorbent–adsorbate equilibrium of the system. The results of Pb^{2+} and Cu^{2+} removal at different adsorbent doses are shown in Figure 5. The adsorption of heavy metal ions generally increased as the adsorbent dose increased.

The results revealed that Pb^{2+} removal rates reached 97.81 ± 0.23% (4.07 ± 0.01 mg/g) and 74.20 ± 0.95% (3.09 ± 0.04 mg/g) for the KN-Ac and KN adsorbents,

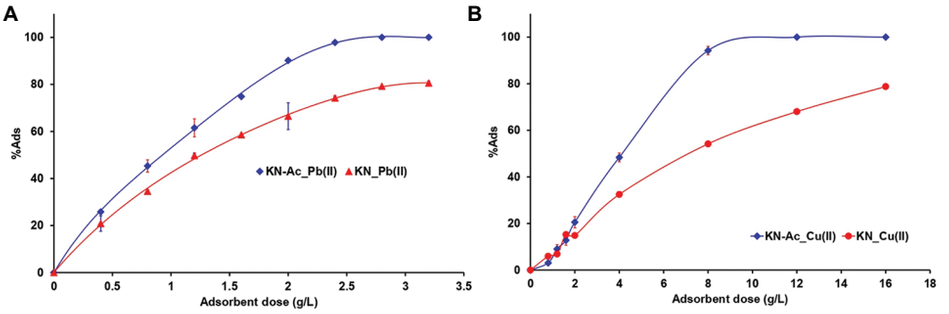

Figure 5. Effect of adsorbent dose of KN-Ac and KN adsorbents on the adsorption (Ads) of (A) lead (Pb[II]) and (B) copper (Cu[II])
Abbreviations: KN: Raw laterite; KN-Ac: Activated laterite.

respectively, when the adsorbent dose was 2.4 g/L. For Cu^{2+}, the adsorption rates were 94.24 ± 1.81% (1.18 ± 0.02 mg/g) and 54.18 ± 0.01% (0.68 ± 0.01 mg/g) for KN-Ac and KN, respectively, when the adsorbent dose was 8 g/L.

When the amount of KN-Ac was increased beyond 2.4 g/L or 8 g/L, the removal rates of Pb^{2+} and Cu^{2+} reached 100%, indicating that most heavy metals in the solution were removed. This demonstrates that acid-treated laterite possesses a strong sorption capacity for Pb^{2+} and Cu^{2+}.

Laterite is characterized by the presence of numerous surface groups, such as ≡*Si-O-H*, ≡*Al-O-H*, and ≡*Fe-O-H*, which play an important role in the sorption of $Pb^{2+}$and Cu^{2+} ions, particularly in slightly acidic or neutral environments. The sorption reaction can be summarized by Equations 7 and 8.

$$\equiv S\text{-}O\text{-}H + Pb^{2+} \longrightarrow \equiv S\text{-}O\text{-}Pb^{+} + H^{+} \quad (7)$$

$$\equiv S\text{-}O\text{-}H + Cu^{2+} \longrightarrow \equiv S\text{-}O\text{-}Cu^{+} + H^{+} \quad (8)$$

where *S* represents silicon (Si), aluminum (Al), or Fe.

The adsorption of solutes onto solid particles involves several main steps: (i) Transport of the solute from the liquid phase to the adsorbent surface; (ii) migration to active sites through ion exchange; and (iii) uptake at these sites through mechanisms, such as complexation, sorption, precipitation, or hydrolysis.[1] As the laterite dose increases, the removal of Pb^{2+} and Cu^{2+} also increases. This phenomenon may be attributed to the greater number of functional groups on the laterite surface, providing more sites available for complex formation through surface complexation or for cation exchange.[46,54,56]

This study aimed to evaluate the adsorption capacity of natural lateritic materials modified with HCl as an alternative to costly adsorbents for removing Cu^{2+} and Pb^{2+} from water. Adsorption capacities of 4.07 ± 0.01 mg/g and 1.18 ± 0.02 mg/g were obtained for Pb^{2+} and Cu^{2+}, respectively. Similar results have been reported by other researchers. For example, Nguyen reported that lateritic soils exhibit adsorption capacities of 1.0–1.2 mg/g for Pb and 0.5–0.8 mg/g for Cu at pH 5.[57] The researcher concluded that although the Cu adsorption capacity is lower than that of Pb, it remains acceptable for water treatment. In a similar approach utilizing local materials in water treatment, activated bentonite was used to remove Pb^{2+} from water, with a maximum adsorption capacity of 1.73 mg/g.[56] Based on these results, the adsorption capacity of the modified laterite examined in this study is acceptable for water treatment.

3.2.4. Influence of initial adsorbate concentration

The adsorption percentages of Pb^{2+} and Cu^{2+} at different initial concentrations by the KN-Ac and KN adsorbents are shown in Figure 6. At an initial concentration of 5 mg/L of Pb^{2+}, the adsorption efficiencies were 99.99% (2.08 mg/g) and 84.91% (1.77 mg/g) for KN-Ac and KN, respectively. For Cu^{2+} (5 mg/L), the removal efficiencies were 99.99% (2.08 mg/g) and 77.08% (1.61 mg/g) for KN-Ac and KN, respectively. It is evident that the percentage of adsorption decreases as the concentration of metal ions in solution increases. However, the removal efficiency stabilizes once a particular concentration threshold is reached.

This decrease can be explained by: (i) The reduction in surface energy due to the occupation of active sites as adsorption progresses on the laterite surface; and (ii) increased cohesive forces between adsorbed metal ions and free metal ions in solution, leading to the release of ions from the adsorbed surface back into the solution.[47,58] Consequently, as the concentration gradient increases and more ions accumulate per unit of adsorbent, the adsorbent reaches saturation. The ions remaining in the solution are therefore no longer adsorbed.[46]

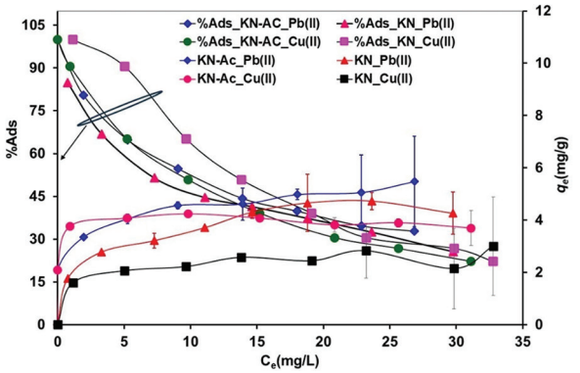

Figure 6. Influence of initial metal concentrations on the removal efficiency of lead (Pb[II]) and copper (Cu[II]) using activated laterite (KN-Ac) and raw laterite (KN)

Notes: q_e: The amount of metal adsorbed per unit mass of adsorbent at equilibrium. ce is the metal ion concentration at equilibrium.

3.2.5. Adsorption isotherm models

The Langmuir, Freundlich, and Temkin isotherms were employed to analyze the adsorption of heavy metals onto the lateritic adsorbents. The linear equations of these models are presented in Equations 9-11.[42,47,54]

$$\frac{C_e}{q_e} = \frac{1}{q_m \times K_L} + \frac{1}{q_m} \times C_e \quad (9)$$

$$lnq_e = lnK_F + \frac{1}{n} \times lnC_e \quad (10)$$

$$q_e = \frac{R \times T}{b_T} lnK_T + \frac{R \times T}{b_T} lnC_e \quad (11)$$

where q_e (mg/g) represents the amount of Pb^{2+} or Cu^{2+} adsorbed at equilibrium and c_e (mg/L) is the equilibrium concentration. q_m (mg/g) is the Langmuir maximum adsorption capacity, and K_L (L/mg) is the Langmuir constant. K_F (L/g) and n are the Freundlich constants corresponding to adsorption capacity and adsorption intensity, respectively. K_T is the Temkin binding constant (L/mg), and b_T is the Temkin constant associated with the heat of adsorption (kJ/mol).

Table 2 shows the parameters calculated from the Langmuir, Freundlich, and Temkin isotherms (Figure 7). These models were selected for their comprehensive description of the adsorption process. Adsorption was best described by the Langmuir isotherm, which exhibited higher coefficients of determination (R^2) than the Freundlich and Temkin models. This suggests that adsorption occurs on a homogeneous surface of the adsorbent, where heavy metal ions diffuse through the pores and channels of the material to replace exchangeable cations in the laterite.[52]

The agreement of the experimental findings with the Langmuir model indicates monolayer adsorption of cations on the outer surface of the adsorbent, reinforcing the role of electrostatic forces in driving monolayer adsorption on the heterogeneous substrate.[50,52,59]

From the Temkin isotherms (Figure 7C), the values of the Temkin constant (b_T) related to the heat of sorption, are listed in Table 2. For Pb^{2+}, the values were approximately 3.26 kJ/mol and 2.76 kJ/mol for KN-Ac and KN, respectively. For Cu^{2+}, the b_T values were 4.73 kJ/mol and 6.03 kJ/mol for KN-Ac and KN, respectively. These low values indicate that the binding energies correspond to physical adsorption for both Pb^{2+} and Cu^{2+}. Similar results were reported by Khater et *al*.[54] for the adsorption of Pb^{2+} and Cu^{2+} on activated carbon, with Temkin constants of 1.046 kJ/mol and 0.241 kJ/mol, respectively.

In addition to the Langmuir, Freundlich, and Temkin models, the Dubinin–Radushkevich model was applied to confirm whether adsorption was chemical or physical. This isotherm is described by Equation 12,[60,61]

$$lnQ = lnQ_m - k \times \varepsilon^2 \quad (12)$$

where Q is the equilibrium adsorption capacity (mg/g), Qm is the maximum capacity (mg/g), and k is the activity coefficient related to the average free energy of adsorption (mol^2/kJ^2). is the Polanyi potential(kJ/mol)andisdefinedas: $\varepsilon = RT\ln\left[1+\left(1/C_e\right)\right]$

where R is the universal gas constant (8.314 J/mol·K), T is the temperature in Kelvin (K), and C_e is the equilibrium concentration of the adsorbate in the aqueous phase (mg/L).

The average adsorption energy E (kJ/mol) was calculated from k using Equation 13.[61]

$$E = -\sqrt{\left(1/2k\right)} \quad (13)$$

If E is between 8 and 16 kJ/mol, adsorption proceeds via ion exchange; if E < 8 kJ/mol, the adsorption is physical.[60,61] The calculated values of E and Qm are presented in Table 2. All E values are <8 kJ/mol, indicating that the adsorption mechanism in this study is physisorption.

3.2.6. Influence of pH

One crucial factor in the adsorption of heavy metals onto adsorbents is the pH of the aqueous solution. The pH

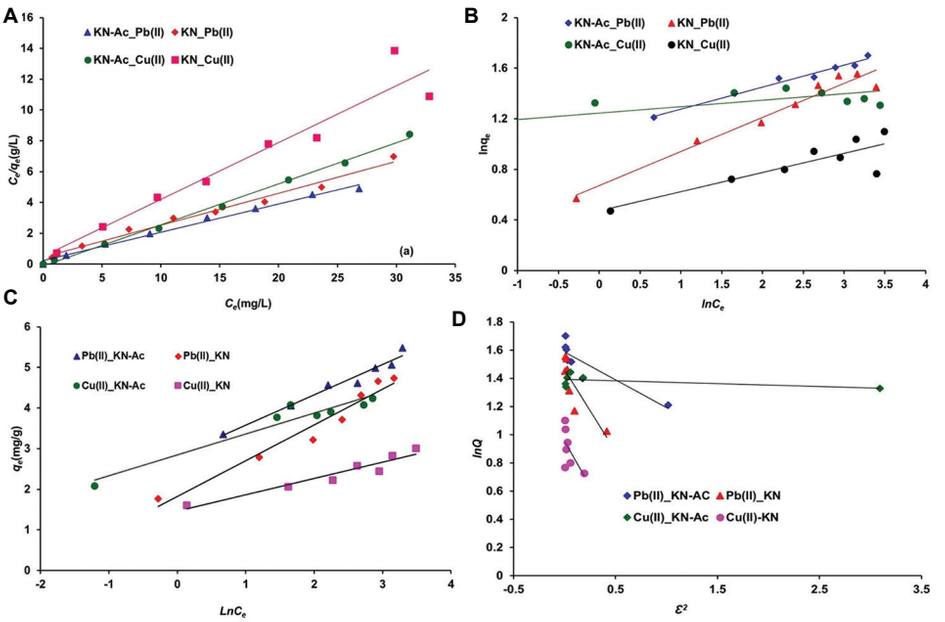

Figure 7. Adsorption isotherm models for lead (Pb[II]) and copper (Cu[II]): (A) Langmuir, (B) Freundlich, (C) Temkin, and (D) Dubinin–Radushkevich

Notes: q_e = The amount of metal adsorbed per unit mass of adsorbent at equilibrium. c_e is the metal ion concentration at equilibrium. is the Polanyi potential (kJ/mol). Q is the equilibrium adsorption capacity (mg/g).
Abbreviations: KN: Raw laterite; KN-Ac: Activated laterite.

can alter the forms in which metal ions exist in solution and affect the chemical and physical characteristics of the adsorbents. Figure 8 illustrates the effect of pH on the removal of Pb^{2+} and Cu^{2+} ions by the KN-Ac and KN adsorbents. As shown in Figure 8, the adsorption rates of both metal ions increase significantly with increasing pH. At pH < 5, the surfaces of the adsorbents are positively charged. The predominance of Pb^{2+} and Cu^{2+} ions in this low pH range creates unfavorable conditions for adsorption. On one hand, electrostatic repulsion between the positively charged metal ions and the adsorbent surface limits adsorption. On the other hand, surface protonation, caused by competition from H_3O^+ ions for binding sites, also contributes to the reduced adsorption.[38,42,50,54] However, at pH > 5, the surface becomes negatively charged, facilitating the adsorption of positively charged metal ions and reaching removal percentages of 65–99% at a pH 6.

At pH 2, the adsorption rate of Pb(II) was 19.62 ± 0.2% (0.82 ± 0.01 mg/g) and 5.78 ± 0.13% (0.24 ± 0.01 mg/g) for the KN-Ac and KN adsorbents, respectively. For Cu(II), the adsorption rate was 12.53 ± 3.32% (0.16 ± 0.04 mg/g) and 1.89 ± 0.05% (0.020 ± 0.001 mg/g) for KN-Ac and KN, respectively. At these low pH values, the concentrations of H_3O^+ ions are much higher than those of Pb^{2+} and Cu^{2+}; consequently, H_3O^+ ions compete with the metal ions for the adsorbent surface, preventing the metals from reaching the binding sites.[24,42] As the pH increased toward 6, the adsorption values rose to approximately 65–99%. This increase reflects the formation of more negatively charged surface sites on the solid, associated with deprotonated silanol (≡*Si-O*-) or aluminol (≡*Al-O*-) species.[21] The enhanced adsorption may be attributed to the decrease in H_3O^+concentration, surface electronegativity, and lower electrostatic repulsion.[24,50]

The adsorption mechanism of Pb^{2+} and Cu^{2+} metals on KN-Ac and KN adsorbents mainly involves ion exchange and outer-sphere complexation. Heavy metal ions replace Fe^{3+} and Al^{3+} ions at exchangeable sites. Additionally, these metals may bind to terminal Al-OH, Fe-OH, and Si-OH groups via inner- or outer-sphere complexation, releasing protons (H^+) in the process.[50,62]

3.2.7. Influence of temperature

A temperature range from 303 K to 333 K was used to determine the temperature dependency of Pb^{2+} and Cu^{2+} adsorption (Figure 9). A positive response in adsorption percentage was observed with increasing temperature up to 333 K. The uptake rates of Pb^{2+} were 97.25 ± 0.73%

Table 2. Langmuir, Freundlich, Temkin, and Dubinin–Radushkevich isotherm parameters for the adsorption of heavy metals by KN-Ac and KN

Isotherm model	Adsorbents	Metals	Parameters		
			Q_m (mg/g)	K_L (L/mg)	R^2
Langmuir	KN-Ac	Pb (II)	5.45	0.75	0.99
	KN	Pb (II)	4.83	0.45	0.98
	KN-Ac	Cu (II)	3.81	2.15	0.99
	KN	Cu (II)	2.71	0.73	0.92
			K_F	n	R^2
Freundlich	KN-Ac	Pb (II)	3.01	5.74	0.97
	KN	Pb (II)	1.96	3.71	0.95
	KN-Ac	Cu (II)	3.47	19.57	0.89
	KN	Cu (II)	1.60	6.60	0.73
			b_T (kJ/mol)	K_T (mg/g)	R^2
Temkin	KN-Ac	Pb (II)	3.26	44.12	0.97
	KN	Pb (II)	2.76	7.91	0.95
	KN-Ac	Cu (II)	4.73	251.04	0.92
	KN	Cu (II)	6.03	38.94	0.92
			Q_m (mg/g)	E (kJ/mol)	R^2
Dubinin–Radushkevich	KN-Ac	Pb (II)	4.89	1.13	0.79
	KN	Pb (II)	4.31	0.66	0.73
	KN-Ac	Cu (II)	4.02	4.98	0.31
	KN	Cu (II)	2.59	0.53	0.37

Notes: E is the average adsorption energy. Q_m is the maximum capacity. b_T is the Temkin constant. R^2 is the determination coefficient. K_L is the Langmuir constant. K_F and n are the Freundlich constants corresponding to adsorption capacity and adsorption intensity, respectively. K_T is the Temkin binding constant.
Abbreviations: KN: Raw laterite; KN-Ac: Activated laterite; Cu (II): Copper; Pb (II): Lead.

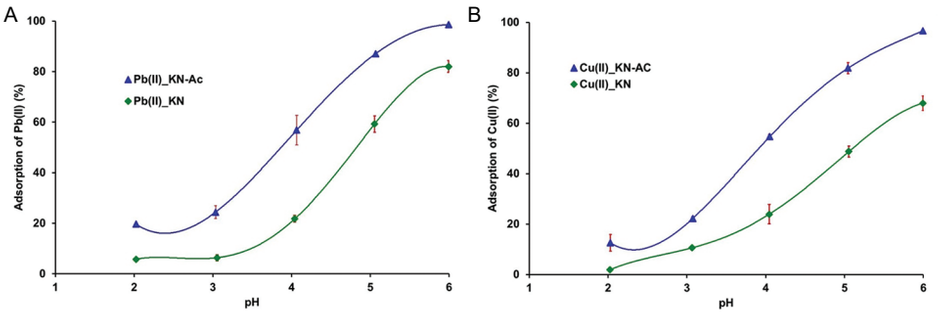

Figure 8. Effect of pH on the percentage adsorption of (A) lead (Pb[II]) and (B) copper (Cu[II]) by activated laterite (KN-Ac) and raw laterite (KN) adsorbents

(4.05 ± 0.03 mg/g) and 73.4 ± 2.1% (3.06 ± 0.08 mg/g) at 303K, rising to 98.79 ± 0.2% (4.12 ± 0.01 mg/g) and 78.60± 0.11% (3.27 ± 0.01 mg/g) at 333K for KN-Ac and KN, respectively. For Cu^{2+}, the adsorption rates increased from 94.74 ± 0.1% (0.118 ± 0.001 mg/g) and 57.58 ± 0.04% (0.72 ± 0.001 mg/g) at 303 K to 96.62 ± 0.13% (1.21 ± 0.001 mg/g) and 64.20 ± 2.31% (0.80 ± 0.02 mg/g) at 333 K for KN-Ac and KN, respectively. The increase in removal rate with temperature indicates an endothermic adsorption process.

The enhanced adsorption at higher temperatures may be attributed to an increased number of available active sites on the laterite surface or improved mobility of metal ions in solution.[44,63]

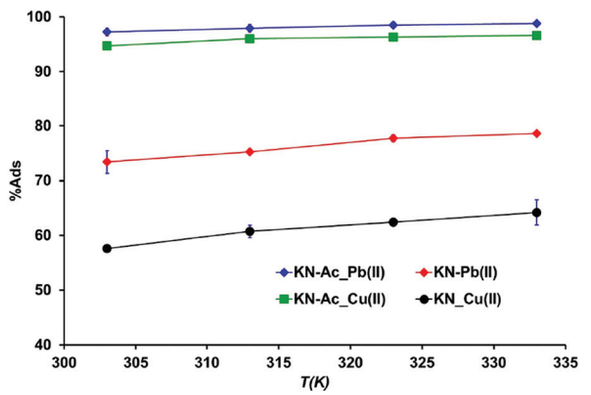

Figure 9. Effect of temperature on the adsorption (Ads) rate of lead (Pb[II]) and copper (Cu[II]) on activated laterite (KN-Ac) and raw laterite (KN)

3.2.8. Thermodynamic parameters

The thermodynamic characteristics of the system—including energy and entropy changes—were evaluated to further interpret the adsorption process. The spontaneity of adsorption depends on changes in Gibbs free energy (ΔG, kJ/mol), enthalpy (ΔH, kJ/mol), and entropy (ΔS, kJ/mol K). These thermodynamic parameters were determined using Equations 14-18. To calculate the parameters, K_d must be dimensionless, and thus K_e was multipliedby the density of water.[53,64]

$$K_e = \left(\frac{C_0 - C_e}{m}\right) \times \frac{V}{C_e} = \frac{q_e}{C_e} \quad (14)$$

$$K_d = K_e \times \rho_e \quad (15)$$

$$\Delta G = -RTlnK_d \quad (16)$$

$$\Delta G = \Delta H - T\Delta S \quad (17)$$

$$lnK_d = \frac{\Delta S}{R} - \frac{\Delta H}{R} \times \frac{1}{T} \quad (18)$$

Here, T is the absolute temperature (K), R is the universal gas constant (8.314 $J/mol.K$), K_e is the ratio of adsorption capacity at equilibrium (L/g), and K_d is the adsorption distribution coefficient.

Figure 10 displays the thermodynamic parameters for metal ion adsorption on the adsorbents. Evaluation of the intercept $\left(\frac{\Delta S}{R}\right)$ and slope $\left(-\frac{\Delta H}{R}\right)$ of the plot of lnK_d as a function of $\left(\frac{1}{T}\right)$ provides the values of ΔS and ΔH.

The ΔG values obtained for all metal ions were negative, suggesting that the adsorption of Pb^{2+} and Cu^{2+} onto KN-Ac and KN is spontaneous and thermodynamically favorable. The order of thermodynamic stability was: Pb^{2+} (KN-Ac) > Cu^{2+} (KN-Ac) > Pb^{2+} (KN) > Cu^{2+} (KN) (Table 3).

The value of ΔH helps distinguish the physicochemical nature of the adsorption. Physisorption typically occurs when ΔH is between 0 and 40 kJ/mol, while chemisorption occurs when ΔH exceeds 40 kJ/mol.[44,53] In this study, all enthalpy values (ΔH) were positive, indicating that the adsorption of metal ions on KN-Ac and KN is endothermic. All values were below 40 kJ/mol, suggesting that physisorption dominates the adsorption mechanism. The positive ΔS values reflect an increase in disorder at the solid–liquid interface during adsorption, likely due to the release of water molecules from the adsorbent surface.[47,54]

Similar results have been reported in the literature by Zhu et *al*.[50] for the removal of heavy metals from wastewater using lateritic ceramics, by Abbou et *al*.[44] for Pb, Cu, and Cd adsorption on natural clay, and by Ozdes et *al*.[63] for Cd(II) and Pb(II) adsorption using Turkish illitic clay.

3.2.9. Co-adsorption of Pb^{2+} and Cu^{2+}

The adsorbents KN-Ac and KN were used to remove heavy metals from an aqueous solution containing a mixture of Pb^{2+} and Cu^{2+} at 10 mg/L, using 2.4 g/L of adsorbents, as shown in Figure 11. The adsorbents exhibited a lower affinity for the mixture of heavy metals.

The adsorption rate of Pb^{2+}, which was 97.81 ± 0.23% in the single-metal system, decreased to 54.85 ± 1.81% in the mixture for KN-Ac, and from 74.20 ± 0.95% to 46.69 ± 0.07% for KN. For Cu^{2+}, the adsorption rate decreased from 48.37± 1.90 to 21.70 ± 1.39% and from 32.46 ± 0.01% to 17.30 ± 0.46% in the binary system for KN-Ac and KN, respectively. The ability of the adsorbents to retain Pb^{2+} remained greater than that for Cu^{2+} in both single and binary systems. Although the ionic radius of Pb^{2+} (1.20 Å) is larger than that of Cu^{2+} (0.73 Å), adsorption is primarily influenced by the hydrated ionic radius. Thus, the observed decrease in adsorption in the binary system (Pb^{2+} + Cu^{2+}) may be related to differences in hydrated ionic radius, favoring a higher proportion of Pb^{2+}.[42]

Table 3. Thermodynamic parameters for the adsorption of Pb(II) and Cu(II) by KN-Ac and KN

Laterite type	ΔG (kJ/mol)				ΔH (kJ/mol)	ΔS (kJ/mol *K*)	R^2
	303 K	313 K	323 K	333 K			
Pb (II)							
KN-Ac	−37,119.2	−51,936.9	−72,494.6	−94,182.6	23.61	0.16	0.99
KN	−17.7	−18.6	−19.5	−20.3	8.34	0.09	0.98
Cu (II)							
KN-Ac	−19.4	−20.7	−21.7	−22.6	12.32	0.10	0.90
KN	−12.9	−13.7	−14.3	−14.9	7.64	0.06	0.98

Notes: ΔG: Gibbs free energy; ΔH: Enthalpy; ΔS: Entropy. R^2 is the determination coefficient.
Abbreviations: KN: Raw laterite; KN-Ac: Activated laterite; Cu(II): Copper; Pb(II): Lead.

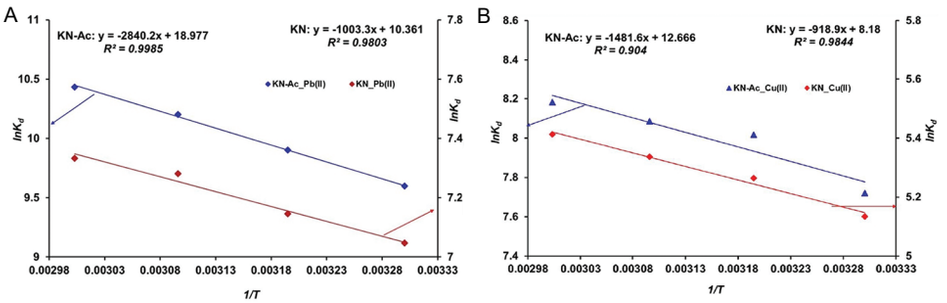

Figure 10. Plot of lnK_d as a function of 1/T for estimating thermodynamic parameters for the adsorption of (A) lead (Pb[II]) and (B) copper (Cu[II]) on activated laterite (KN-Ac) and raw laterite (KN)
Note: K_d is the adsorption distribution coefficient; T is the absolute temperature (K)

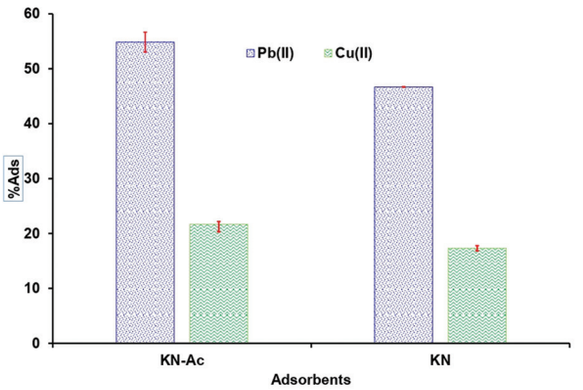

Figure 11. Removal rates of lead (Pb[II]) and copper (Cu[II]) from an aqueous solution containing a mixture of heavy metals
Abbreviations: Ads: Adsorption; KN: Raw laterite; KN-Ac: Activated laterite.

3.3. Interaction of Pb^{2+} and Cu^{2+} with KN-Ac and KN adsorbents

The FTIR spectra of KN and KN-Ac before and after adsorption of Pb^{2+} and Cu^{2+} are shown in Figure 12. The FTIR spectra of KN display bands around 3,695 cm^{-1} [13,17,65,66] and 3,618 cm^{-1}, attributed to hydroxyl groups (-OH). The absorption band at 3,430 cm^{-1} is attributed to groups in Fe, Al, and Si minerals, while the band around 1,639 cm^{-1} corresponds to water molecules in the inner layer.[17,66] The bands at 1,110, 1,033, 914, and 786 cm^{-1} arise from Si-O-Fe, Al-OH, Fe-OH vibrations.[17,66,67] The bands at 536 and 470 cm^{-1} correspond to Fe-O stretching in hematite.[17,66,68] Following metal ion adsorption, the spectra preserved the main functional groups, including Si-O-Fe (1,110 cm^{-1}), Si-O-Si (1,033 cm^{-1}), Al-OH (914 cm^{-1}), Fe-OH (786 cm^{-1}), and -OH (3,695–3,430 cm^{-1}). Furthermore, slight decreases in peak intensities were observed for KN-Ac after adsorption of heavy metals compared to the modified laterite (KN-Ac). For KN + heavy metals, no significant changes in peak intensities were observed. These slight decreases may be due to the low initial concentration of heavy metals used during adsorption.

Fourier transform infrared spectra alone are insufficient to conclusively determine the adsorption mechanism, that is, to confirm or refute whether Pb^{2+} or Cu^{2+} ions were chemically adsorbed onto the lateritic materials containing Fe and Al.

Similar observations were reported by Zhu et *al*.[50] using ceramic laterite for heavy metal removal and by Chatterjee

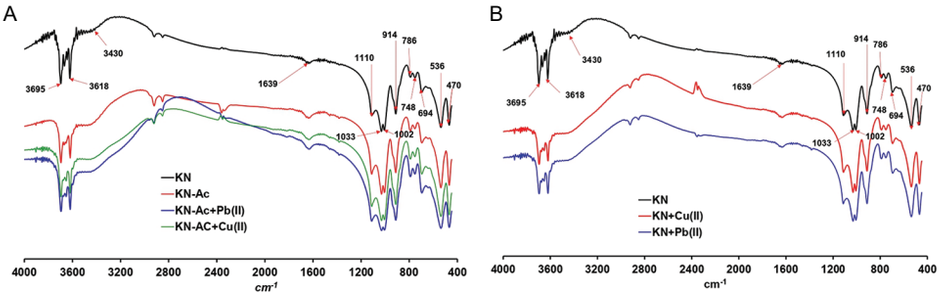

Figure 12. Fourier transform infrared spectroscopy of (A) KN, KN-Ac, and KN-Ac loaded with heavy metals; and (B) KN and KN loaded with heavy metals

Abbreviations: Cu(II): Copper; KN: Raw laterite; KN-Ac: Activated laterite; Pb(II): Lead

and De[38] and He *et al.,*[19] who also noted attenuated peak intensities after Pb^{2+} adsorption onto laterites.

4. Conclusion

Based on the experimental results, both chemically treated and untreated KN possess surface functional groups ((≡Si-O-H, ≡Al-O-H, and ≡Fe-O-H) that play an important role in the sorption of Pb^{2+} and Cu^{2+} metal ions from aqueous solutions.

Maximum removal was observed at 2.4 g/L of KN-Ac for Pb^{2+} and 8 g/L for Cu^{2+}. At pH > 5, the adsorbent surface becomes negatively charged, facilitating the adsorption of positively charged metal ions, with removal percentages reaching 65–99% at pH 6. Pb^{2+} and Cu^{2+} ions were retained by laterite minerals, such as Fe_2O_3 and Al_2O_3 through specific adsorption mechanisms. These ions were adsorbed onto terminal OH groups, such as Fe-OH and Al-OH on the mineral surfaces.

Adsorption was best described by the Langmuir isotherm, which exhibited higher coefficients of determination (R^2) than the Freundlich and Temkin models. This suggests that adsorption occurs on a homogeneous surface, where heavy metal ions must diffuse through pores and channels to replace exchangeable cations, such as Ca^{2+}, Mg^{2+}, potassium ions (K^+), and sodium ions (Na^+) in the laterite structure.

The maximum adsorption capacities of KN-Ac for Pb(II) and Cu(II)—according to the Langmuir model—were 5.45 mg/g and 3.81 mg/g, respectively, both higher than the values for KN, which were 4.83 mg/g and 2.71 mg/g.

The adsorption of Pb^{2+} and Cu^{2+} on KN-Ac and KN is mainly due to physisorption, as demonstrated by the E values obtained from the Dubinin–Radushkevich model and by the low Temkin constants (b_T), further supported by the thermodynamic parameters and FTIR spectra of post-adsorption residues.

The negative ΔG values for all metal ions indicate that the adsorption of Pb(II) and Cu(II) is spontaneous and thermodynamically feasible on both KN-Ac and KN, following the order of stability: Pb^{2+} (KN-Ac) > Cu^{2+} (KN-Ac) > Pb^{2+} (KN) > Cu^{2+} (KN). All ΔH values were positive and below 40 kJ/mol, confirming the endothermic nature of adsorption and the predominance of physisorption.

In future work, we aim to further investigate specific adsorption mechanisms using additional techniques, such as X-ray photoelectron spectroscopy or transmission electron microscopy, energy-dispersive X-ray spectroscopy to reduce the uncertainty associated with interpretations based on the pseudo-second-order model, the Dubinin–Radushkevich model, and FTIR spectra, which collectively suggest the dominance of physical adsorption.

Acknowledgments

The authors thank the following services for their assistance: the Chemical and Biochemical Engineering Department and the Thermodynamic and Physical Mathematics Department of the University of Mons (Belgium).

Funding

The authors thank the Academic of Research and Higher Education–Commission of Development Cooperation/ Mons 2024 (Belgium; grant number: 2024/25) and the International Science Program (Uppsala, Sweden, grant number: BUF 02) for their financial support.

Conflict of interest

The authors declare that they have no competing interests.

Author contributions

Conceptualization: All authors
Investigation: Corneille Bakouan
Methodology: All authors
Writing – original draft: Corneille Bakouan
Writing–review & editing: All authors

Availability of data

The data supporting this study are available from the corresponding author upon justified request.

References

1. Pyrgaki K, Messini P, Zotiadis V. Adsorption of Pb and Cu from aqueous solutions by raw and heat-treated attapulgite clay. *Geosciences*. 2018;8(5):157. doi: 10.3390/geosciences8050157
2. Bo S, Luo J, An Q, Xiao Z, Wang H, Shangru ZL. Efficiently selective adsorption of Pb(II) with functionalized alginate-based adsorbent in batch/column systems: Mechanism and application simulation. *J Clean Prod*. 2020;250:119585. doi: 10.1016/j.jclepro.2019.119585
3. Chowdhury IR, Chowdhury S, Mazumder MAJ, Al-Ahmed A. Removal of lead ions (Pb^{2+}) from water and wastewater: A review on the low-cost adsorbents. *Appl Water Sci.* 2022;12(8):185. doi: 10.1007/s13201-022-01703-6
4. Hama AKH, Mustafa FS, Omer KM, Hama S, Hamarawf RF, Rahman KO. Heavy metal pollution in the aquatic environment: Efficient and low-cost removal approaches to eliminate their toxicity: A review. *RSC Adv*. 2023;13(26):17595-17610. doi: 10.1039/D3RA00723E
5. Zhao S, Chen K, Xiong B, Guo C, Dang Z. Prediction of adsorption of metal cations by clay minerals using machine learning. *Sci Total Environ*. 2024;924:171733. doi: 10.1016/j.scitotenv.2024.171733
6. Khalfa L, Sdiri A, Bagane M, Cervera ML. A calcined clay fixed bed adsorption studies for the removal of heavy metals from aqueous solutions. *J Clean Prod.* 2021;278:123935. doi: 10.1016/j.jclepro.2020.123935
7. Moradpour S, Entezari M, Ayoubi S, Karimi A, Naimi S. Digital exploration of selected heavy metals using Random Forest and a set of environmental covariates at the watershed scale. *J Hazard Mater*. 2023;455:131609. doi: 10.1016/j.jhazmat.2023.131609
8. Muthu M, Sadowski L. Heavy metals removal in a graphene engineered concrete-based filter column. *J Build Eng.* 2024;91:109583. doi: 10.1016/j.jobe.2024.109583
9. Gu S, Kang X, Wang L, Lichtfouse E, Wang C. Clay mineral adsorbents for heavy metal removal from wastewater: A review. *Environ Chem Lett*. 2019;17(2):629-654. doi: 10.1007/s10311-018-0813-9
10. Mritunjay, Quaff AR. Adsorption of copper on activated Ganga sand from aqueous solution: Kinetics, isotherm, and optimization. *Int J Environ Sci Technol*. 2022;9(10):9679-9690. doi: 10.1007/s13762-021-03651-1
11. Alghamdi AG, Alasmary Z. Fate and transport of lead and copper in calcareous soil. *Sustainability*. 2023;15:775. doi: 10.3390/su15010775
12. Chatterjee S, Mondal S, De S. Design and scaling up of fixed bed adsorption columns for lead removal by treated laterite. *J Clean Prod*. 2018;177:760-774. doi: 10.1016/j.jclepro.2017.12.249
13. Pham TD, Nguyen HH, Nguyen NV, *et al*. Adsorptive removal of copper by using surfactant modified laterite soil. *J Chem.* 2017;2017:1-10. doi: 10.1155/2017/1986071
14. Chatterjee S, Sivareddy I, De S. Adsorptive removal of potentially toxic metals (cadmium, copper, nickel and zinc) by chemically treated laterite: Single and multicomponent batch and column study. *J Environ Chem Eng*. 2017;5(4):3273-3289. doi: 10.1016/j.jece.2017.06.029
15. Uditha N, Dissanayake S, Jayawardana DT, Mapatuna H, Ravilojan H. Thermally modified laterite soil by means of an adsorptive material for copper and chromium elimination from polluted Water. *Chem Environ Sci Arch.* 2023;3(1):8-14. doi: 10.47587/CESA.2023.3102
16. Fouodjouo M, Fotouo-Nkaffo H, Laminsi S, Cassini FA, Brito-Benetoli LO, Debacher NA. Adsorption of copper (II) onto Cameroonian clay modified by non-thermal plasma: Characterization, chemical equilibrium and thermodynamic studies. *Appl Clay Sci*. 2017;142:136-144. doi: 10.1016/j.clay.2016.09.028
17. Mitra S, Thakur LS, Rathore VK, Mondal P. Removal of Pb(II) and Cr(VI) by laterite soil from synthetic waste water: Single and bi-component adsorption approach. *Desalination Water Treat.* 2016;57(39):18406-18416. doi: 10.1080/19443994.2015.1088806
18. Mohapatra M, Khatun S, Anand S. Kinetics and thermodynamics of lead (II) adsorption on lateritic nickel ores of Indian origin. *Chem Eng J*. 2009;155:184-190. doi: 10.1016/j.cej.2009.07.035
19. He F, Ma B, Wang C, Chen Y, Hu X. Adsorption of Pb(II) and Cd(II) hydrates via inexpensive limonitic laterite: Adsorption characteristics and mechanisms. *Sep Purif Technol*. 2023;310:123234. doi: 10.1016/j.seppur.2023.123234
20. Budsaereechai S, Kamwialisak K, Ngernyen Y.

Adsorption of lead, cadmium and copper on natural and acid activated bentonite clay. *KKU Res J*. 2012;17(5):800-810.
21. Sandy, Maramis V, Kurniawan A, Ayucitra A, Sunarso J, Ismadji S. Removal of copper ions from aqueous solution by adsorption using LABORATORIES-modified bentonite (organo-bentonite). *Front Chem Sci Eng*. 2012;6(1):58-66. doi: 10.1007/s11705-011-1160-6
22. Mhamdi M, Galai H, Mnasri N, Elaloui E, Trabelsi-Ayadi M. Adsorption of lead onto smectite from aqueous solution. *Environ Sci Pollut Res*. 2013;20(3):1686-1697. doi: 10.1007/s11356-012-1015-9
23. Chaari I, Fakhfakh E, Chakroun S, *et al*. Lead removal from aqueous solutions by a Tunisian smectitic clay. *J Hazard Mater*. 2008;156:545-551. doi: 10.1016/j.jhazmat.2007.12.080
24. Olgun A, Atar N. Equilibrium, thermodynamic and kinetic studies for the adsorption of lead (II) and nickel (II) onto clay mixture containing boron impurity. *J Ind Eng Chem*. 2012;18(5):1751-1757. doi: 10.1016/j.jiec.2012.03.020
25. Resmi G, Thampi SG, Chandrakaran S. Removal of lead from wastewater by adsorption using acid-activated clay. *Environ Technol*. 2012;33(3):291-297. doi: 10.1080/09593330.2011.572917
26. Al-Jlil SA, Alsewailem FD. Saudi Arabian clays for lead removal in wastewater. *Appl Clay Sci.* 2009;42:671-674. doi: 10.1016/j.clay.2008.03.012
27. Es-Sahbany H, Hsissou R, El Hachimi ML, Allaoui M, Nkhili S, Elyoubi MS. Investigation of the adsorption of heavy metals (Cu, Co, Ni and Pb) in treatment synthetic wastewater using natural clay as a potential adsorbent (Sale-Morocco). *Mater Today Proc.* 2021;45:7290-7298. doi: 10.1016/j.matpr.2020.12.1100
28. Rakhym AB, Seilkhanova GA, Kurmanbayeva TS. Adsorption of lead (II) ions from water solutions with natural zeolite and chamotte clay. *Mater Today Proc.* 2020;31:482-485. doi: 10.1016/j.matpr.2020.05.672
29. Oubagaranadin JUK, Murthy ZVP. Adsorption of divalent lead on a montmorillonite-illite type of clay. *Ind Eng Chem Res.* 2009;48(23):10627-10636. doi: 10.1021/ie9005047
30. Chen C, Liu H, Chen T, Chen D, Frost RL. An insight into the removal of Pb(II), Cu(II), Co(II), Cd(II), Zn(II), Ag(I), Hg(I), Cr(VI) by Na(I)-montmorillonite and Ca(II)-montmorillonite. *Appl Clay Sci.* 2015;118:239-247. doi: 10.1016/j.clay.2015.09.004
31. Kushwaha A, Rani R, Patra JK. Adsorption kinetics and molecular interactions of lead [Pb(II)] with natural clay and humic acid. *Int J Environ Sci Technol.* 2020;17(3):1325-1336. doi: 10.1007/s13762-019-02411-6
32. Sudha Rani K, Srinivas B, Gourunaidu K, Ramesh KV. Removal of copper by adsorption on treated laterite. *Mater Today Proc.* 2018;5(1):463-469. doi: 10.1016/j.matpr.2017.11.106
33. Federal T, Ilaro P, State O, State O. Sorption of competing heavy metals on laterite. *FEPI JOPAS*. 2023;5(1):1-9.
34. Ouedraogo RD, Bakouan C, Sorgho B, Guel B, Bonou LD. Characterization of a natural laterite of Burkina Faso for the elimination of arsenic (III) and arsenic (V) in groundwater. *Int J Biol Chem Sci*. 2019;13(6):2959-2977. doi: 10.4314/ijbcs.v13i6.41
35. Bakouan C. *Caractérisation de Quelques Sites Latéritiques du Burkina Faso: Application à L'élimination de L'arsenic (III) et (V) Dans Les Eaux Souterraines. Ph.D. Thesis, Université de Ouaga I Pr Joseph KI-ZERBO, Ouagadougou, Burkina Faso*. Université de Mons, Mons, Belgium; 2018. p. 1-241. Available from: https://orbi.umons.ac.be/bitstream/20.500.12907/31806/1/Th%C3%A8se [Last accessed on 2018 Feb 01].
36. Bakouan C, Chenoy L, Guel B, Hantson AL. Physicochemical and mineralogical characterizations of two natural laterites from Burkina Faso: Assessing their potential usage as adsorbent materials. *Minerals*. 2025;15(4):379. doi: 10.3390/min15040379
37. Karki S, Timalsina H, Budhathoki S, Budhathoki S. Arsenic removal from groundwater using acid-activated laterite. *Groundw Sustain Dev*. 2021;18:100769. doi: 10.1016/j.gsd.2022.100769
38. Chatterjee S, De S. Application of novel, low-cost, laterite-based adsorbent for removal of lead from water: Equilibrium, kinetic and thermodynamic studies. *J Environ Sci Health A Tox Hazard Subst Environ Eng.* 2016;51(3):193-203. doi: 10.1080/10934529.2015.1094321
39. Chaari I, Moussi B, Jamoussi F. Interactions of the dye, C.I. direct orange 34 with natural clay. *J Alloys Compd*. 2015;647:720-727. doi: 10.1016/j.jallcom.2015.06.142
40. Vasic A, Gulicovski J, Stojmenovic M, *et al*. Removal of ethyl xanthate anions from contaminated aqueous solutions using hazardous waste slag generated by lignite combustion. *Water*. 2024;16:2037. doi: 10.3390/w16142037
41. Rouibah K, Ferkous H, Abdessalam-Hassan M, *et al*. Exploring the efficiency of algerian kaolinite clay in the adsorption of Cr(III) from aqueous solutions: Experimental and computational. *Molecules*. 2024;29(9):2135. doi: 10.3390/molecules29092135
42. Chu Y, Khan MA, Wang F, Xia M, Lei W, Zhu S. Kinetics and equilibrium isotherms of adsorption of Pb(II) and Cu(II) onto raw and arginine-modified montmorillonite. *Adv Powder Technol.* 2019;30(5):1067-1078. doi: 10.1016/j.apt.2019.03.002

43. Wang C, Qiao J, Yuan J, *et al*. Novel chitosan-modified biochar prepared from a Chinese herb residue for multiple heavy metals removal: Characterization, performance and mechanism. *Bioresour Technol.* 2024;402:130830. doi: 10.1016/j.biortech.2024.130830
44. Abbou B, Lebkiri I, Ouaddari H, *et al*. Removal of Cd(II), Cu(II), and Pb(II) by adsorption onto natural clay: A kinetic and thermodynamic study. *Turk J Chem.* 2021;45(2):362-376. doi: 10.3906/kim-2004-82
45. Hussain TS, Khaleefa Ali SA. Removal of heavy metal by ion exchange using bentonite clay. *J Ecol Eng.* 2020;22(1):104-111. doi: 10.12911/22998993/128865
46. Ayach J, Duma L, Badran A, *et al*. Enhancing wastewater depollution: Sustainable biosorption using chemically modified chitosan derivatives for efficient removal of heavy metals and dyes. *Materials (Basel)*. 2024;17(11):2724. doi: 10.3390/ma17112724
47. Dash B, Dash B, Rath SS. A thorough understanding of the adsorption of Ni (II), Cd (II) and Zn (II) on goethite using experiments and molecular dynamics simulation. *Sep Purif Technol.* 2020;240:116649. doi: 10.1016/j.seppur.2020.116649
48. El-Enein SA, Okbah MA, Hussain SG, Soliman NF, Ghounam HH. Adsorption of selected metals ions in solution using nano-bentonite particles: Isotherms and kinetics. *Environ Process.* 2020;7(2):463-477. doi: 10.1007/s40710-020-00430-x
49. Potgieter JH, Potgieter-Vermaak SS, Kalibantonga PD. Heavy metals removal from solution by palygorskite clay. *Miner Eng.* 2006;19(5):463-470. doi: 10.1016/j.mineng.2005.07.004
50. Zhu D, He Y, Zhang B, *et al*. Simultaneous removal of multiple heavy metals from wastewater by novel plateau laterite ceramic in batch and fixed-bed studies. *J Environ Chem Eng.* 2021;9(5):1-9. doi:10.1016/j.jece.2021.105792
51. Nguyen TC, Loganathan P, Nguyen TV, Vigneswaran S, Kandasamy SJ, Naidu R. Simultaneous adsorption of Cd, Cr, Cu, Pb, and Zn by an iron-coated Australian zeolite in batch and fixed-bed column studies. *Chem Eng J.* 2015;270:393-404. doi: 10.1016/j.cej.2015.02.047
52. Qiu Q, Jiang X, Lv G, *et al*. Adsorption of heavy metal ions using zeolite materials of municipal solid waste incineration fly ash modified by microwave-assisted hydrothermal treatment. *Powder Technol*. 2018;335:156-163. doi: 10.1016/j.powtec.2018.05.003
53. Zou C, Jiang W, Liang J, Sun X, Guan Y. Removal of Pb(II) from aqueous solutions by adsorption on magnetic bentonite. *Environ Sci Pollut Res.* 2019;26(2):315-1322. doi: 10.1007/s11356-018-3652-0
54. Khater D, Alkhabbas M, Al-Ma'abreh AM. Adsorption of Pb, Cu, and Ni Ions on activated carbon prepared from oak cupules: Kinetics and thermodynamics studies. *Molecules*. 2024;29(11):2489. doi: 10.3390/molecules29112489
55. Wu S, Xie F, Chen S, Fu B. The removal of Pb (II) and Cd (II) with hydrous manganese dioxide: Mechanism on zeta potential and adsorption behavior. *Environ Technol.* 2020;41(24):3219-3232. doi: 10.1080/09593330.2019.1604814
56. Chuang Y, Chen J, Lu J, *et al*. Sorption studies of Pb(II) onto montmorillonite clay. *IOP Conf Ser Earth Environ Sci*. 2022;1087(1):1087012007. doi: 10.1088/1755-1315/1087/1/012007
57. Nguyen THN. Appication of Laterite Soil to Heavy Metal Treatment in Water. In: *Proceedings of the 19th IAHR-APD Congress 2014, Hanoi, Vietnam*; 2014. p. 1-7.
58. Panda L, Rath SS, Rao DS, Nayak BB, Das B, Misra PK. Thorough understanding of the kinetics and mechanism of heavy metal adsorption onto a pyrophyllite mine waste based geopolymer. *J Mol Liq*. 2018;263:428-441. doi: 10.1016/j.molliq.2018.05.016
59. Zhou Q, Liao B, Lin L, Qiu W, Song Z. Adsorption of Cu(II) and Cd(II) from aqueous solutions by ferromanganese binary oxide-biochar composites. *Sci Total Environ*. 2018;615:115-122. doi: 10.1016/j.scitotenv.2017.09.220
60. Bishwas RK, Mostofa S, Alam MA, Jahan SA. Removal of malachite green dye by sodium dodecyl sulfate modified bentonite clay: Kinetics, thermodynamics and isotherm modeling. *Next Nanotechnol.* 2023;3-4:100021. doi: 10.1016/j.nxnano.2023.100021
61. Mostafapour FK, Yilmaz M, Mahvi AH, Younesi A, Ganji F, Balarak D. Adsorptive removal of tetracycline from aqueous solution by surfactant-modified zeolite: Equilibrium, kinetics and thermodynamics. *Desalination Water Treat.* 2022;247:216-228. doi: 10.5004/dwt.2022.27943
62. Qiu W, Zheng Y. Removal of lead, copper, nickel, cobalt, and zinc from water by a cancrinite-type zeolite synthesized from fly ash. *Chem Eng J.* 2009;145(3):483-488. doi: 10.1016/j.cej.2008.05.001
63. Ozdes D, Duran C, Senturk HB. Adsorptive removal of Cd(II) and Pb(II) ions from aqueous solutions by using Turkish illitic clay. *J Environ Manage*. 2011;92(12):3082-3090. doi: 10.1016/j.jenvman.2011.07.022
64. Frantz TS, Silveira N, Quadro MS, *et al*. Cu(II) adsorption from copper mine water by chitosan films and the matrix effects. *Environ Sci Pollut Res*. 2017;24(6):5908-5917. doi: 10.1007/s11356-016-8344-z
65. Nguyen TH, Tran HN, Vu HA, *et al.* Laterite as a low-cost adsorbent in a sustainable decentralized filtration system to remove arsenic from groundwater in Vietnam.

Sci Total Environ. 2020;699:134267.
doi: 10.1016/j.scitotenv.2019.134267

66. Rathore VK, Dohare DK, Mondal P. Competitive adsorption between arsenic and fluoride from binary mixture on chemically treated laterite. *J Environ Chem Eng.* 2016;4(2):2417-2430.
doi: 10.1016/j.jece.2016.04.017
67. Ghani U, Hussain S, Amin N, Imtiaz M, Ali Khan S. Laterite clay-based geopolymer as a potential adsorbent for the heavy metals removal from aqueous solutions. *J Saudi Chem Soc.* 2020;24(11):874-884.
doi: 10.1016/j.jscs.2020.09.004
68. Nguyen TH, Nguyen AT, Loganathan P, *et al*. Low-cost laterite-laden household filters for removing arsenic from groundwater in Vietnam and waste management. *Process Saf Environ Protect.* 2021;152: 154-163.
doi: 10.1016/j.psep.2021.06.002